deed, they remark that their calculations is not valid for homovalent solutes, so the results for Ag in Cu are presumably also invalid.)

Two features of the consequences of the theory are perhaps not adequately emphasized by the table. The first-neighbor theoretical-field-gradient magnitude is strongly charge dependent, while the experimental values are not. The second-neighbor theoretical gradients are also charge dependent, and the experimental gradients, although lacking Ge and In, seem to depend more strongly on charge. But the quantitative agreement is just as poor as for the first neighbors, being relatively good only for the case of Sb, where $Z'=4$. We have calculated (unpublished) the gradient out to distances from the impurity which include the seventh shell, and find the field gradients to be too small to explain the measured wipeout numbers. That is, the Alfred–Van Ostenberg potentials with the Hurd–Gordon phase shifts are adequate to explain the data in neither the near nor asymptotic regions, whereas simpler approaches,[9] such as Kohn–Vosko, have been more successful in the asymptotic region.

ACKNOWLEDGMENTS

We wish to express our appreciation to Professor Paul Flinn and John Rayne for their excellent advice on sample preparation, and to Professor Larry Vassamillet for the electron-microprobe analysis of the samples.

*Work supported by National Science Foundation Grant No. GP-17559. From Ph.D. thesis of George Schnakenberg, Jr., 1971.

†Present address: United States Bureau of Mines, 4800 Forbes Ave., Pittsburgh, Pa. 15213.

[1]T. J. Rowland, Phys. Rev. **119**, 900 (1960).

[2]A. G. Redfield, Phys. Rev. **130**, 589 (1963).

[3]R. T. Schumacher and George Schnakenberg, Jr., Solid State Commun. **7**, 1735 (1969).

[4]B. L. Jensen, R. Nevald, and D. L. Williams, J. Phys. F **2**, 169 (1972).

[5]J. Friedel, Philos. Mag. 43, 153 (1952).

[6]W. Kohn and S. H. Vosko, Phys. Rev. **119**, 912 (1960).

[7]L. C. R. Alfred and D. O. Van Ostenberg, Phys. Lett. A **26**, 27 (1967).

[8]C. M. Hurd and E. M. Gordon, Phys. Chem. Solids **29**, 2205 (1968).

[9]K. Tompa, G. Grüner, A. Janossy, and F. Toth, Solid State Commun. **7**, 697 (1969).

PHYSICAL REVIEW B VOLUME 7, NUMBER 6 15 MARCH 1973

Lattice Thermal Conductivity in High-Concentration Mixed Crystals*

J. K. Flicker and P. L. Leath
Department of Physics, Rutgers, The State University, New Brunswick, New Jersey 08903
(Received 2 August 1972)

The lattice thermal conductivity in high-concentration harmonic isotopically disordered mixed crystals is calculated within the coherent-potential approximation from the appropriate Kubo formula using the energy current operators of Hardy. The infrared divergence in harmonic systems is eliminated by restriction to finite systems and, in a three-dimensional case, by adding an anharmonic phonon-phonon scattering term. Numerical calculations are performed in one, two, and three dimensions with nearest-neighbor forces for a linear chain, a simple square lattice, and a simple cubic lattice, respectively. In one and two dimensions, comparisons with the computer experiments of Payton *et al.* show qualitative agreement with the concentration dependence of the thermal conductivity at all concentrations although the overall magnitude is larger by factors of about 10.8 and 5.4, respectively. It is observed that low-frequency resonant modes considerably decrease the thermal conductivity.

I. INTRODUCTION

There has been considerable discussion in the literature of the thermal conductivity of disordered systems by several quite distinct approaches, most of them in one-dimensional systems. A useful test of various analytical approaches has been provided by Payton *et al.*,[1] who performed computer experiments on one- and two-dimensional isotopically disordered lattices. They used the classical equations of motion of the lattice atoms to calculate the local energy density and hence the energy flow at one end of their system when the other end of their system was allowed to be in contact with particles having a Maxwellian distribution of velocities. They plotted the thermal conductivity versus concentration of the two isotopic species throughout the concentration range.

Recently, several groups have concerned themselves with the dependence of the lattice thermal conductivity κ of a disordered, harmonic, one-dimensional chain on its number of atoms N. For

example, Casher and Liebowitz have shown[2] that κ diverges linearly with N (for large N) in any harmonic, linear chain where the spectral density has an absolutely continuous part. In light of the results of Matsuda and Ishii[3] (who used a transfer matrix method) and those of Rubin and Greer[4] that $\kappa \sim N^{1/2}$ (for large N), Casher and Liebowitz conclude that, with probability 1, the frequency spectrum of a disordered linear chain has no absolutely continuous part. It is not clear that there is agreement between the N dependence observed in the computer experiments[1] and that in the various theories. In particular, there apparently is a very strong effect of the boundary conditions at the ends of the system.[5]

The purpose of this work is not to ferret out the N dependence in any exact calculation, but to simply proceed via the appropriate Kubo formula and a coherent-potential approximation to calculate the thermal conductivity at all concentrations in harmonic, isotopically disordered alloys in one, two, and three dimensions. The formalism developed is equivalent at low concentrations to that which Woll[6] developed some years ago, using the techniques of Langer.[7]

It is very well known that, for a perfect, infinite, harmonic lattice, the phonons cannot come into thermal equilibrium and hence cannot sustain a thermal gradient, so that the thermal conductivity is infinite. It is less well known, perhaps, that the thermal conductivity is also, it seems, infinite for any infinite, harmonic system regardless of disorder or dimensionality.[8] Whatever disorder may be present simply is not seen by the phonons of much larger wavelengths than the range of disorder; thus since these phonons travel at the speed of sound, there is an infrared divergence in the thermal conductivity. Such a divergence does not occur in the electronic transport problem, since the longer-wavelength electrons move more slowly. This divergence in real systems is removed by finite crystal boundary scattering, anharmonic phonon scattering, etc. In order to view the concentration dependence of the thermal conductivity for harmonic alloys in this paper, in the final calculations we either limit the crystal to an appropriate finite size or add empirically an anharmonic scattering term.[9] Thereby, we obtain qualitative agreement with the concentration dependence of the computer experiments.[1] The deviations from the concentration dependence in the two approaches we attribute to the lack of participation, in part, of low-frequency resonant modes somewhat localized about the heavier atoms.

Specifically, in Sec. II, we evaluate a Kubo formula for the thermal conductivity using the thermal current operator of Hardy.[10] The expression is evaluated in Sec. III using the double-time Green's function of Zubarev[11] in the single-site, self-consistent approximation of Taylor[12] (which is known as the "coherent-potential approximation" in electronic theory[13,14]). The coherent-potential approximation gives a useful formula at all concentrations and is exact at both limits of concentration. In Sec. IV, numerical results are obtained for the cases of one-, two- and three-dimensional systems with nearest-neighbor forces and compared with the computer experiments of Payton *et al.*[1] in one and two dimensions. Finally, the conclusions on the effect of disorder are discussed in Sec. V.

II. FORMULATION OF GENERAL PROBLEM

The Hamiltonian is chosen to be

$$H = \sum_{l,\alpha} \frac{p_\alpha^2(l)}{2M(l)} + \frac{1}{2} \sum_{l,l',\alpha,\beta} \phi_{\alpha\beta}(l, l') u_\alpha(l) u_\beta(l') , \tag{1}$$

where M_l is the mass of the atom at the lth site, $u_\alpha(l)$ and $p_\alpha(l)$ are the displacement and momentum of the lth atom in the αth Cartesian direction, respectively, and $\phi_{\alpha\beta}(l, l')$ is the harmonic force constant. The effect of alloying the isotopes is to make the mass of the lth atom a random variable, while the ϕ's are assumed to be unchanged from those of the pure substance.

A convenient formalism to describe such systems is the retarded, double-time, displacement-displacement Green's function defined by

$$G_{\alpha\beta}(l, l'; t) \equiv \langle\langle u_\alpha(l, t); u_\beta(l', 0)\rangle\rangle$$
$$= 2\pi(i\hbar)^{-1} \theta(t) Z^{-1} \mathrm{Tr}\{e^{-\beta H}[u_\alpha(l, t), u_\beta(l', 0)]\} \tag{2}$$

in the notation of Zubarev,[11] where Z is the partition function, $[\ldots, \ldots]$ is a commutator, and $\theta(t)$ is the Heaviside step function. By differentiating twice with respect to t and Fourier-transforming the time variable, $G_{\alpha\beta}(l, l'; \omega)$ is easily shown to satisfy the equation of motion

$$G_{\alpha\beta}(l, l'; \omega) = P_{\alpha\beta}(l, l'; \omega) + \sum_{n,\gamma} P_{\alpha\gamma}(l, n) V_n G_{\gamma\beta}(n, l'; \omega) , \tag{3a}$$

where $V_n = m_0 \epsilon_n \omega^2$, $\epsilon_n = 1 - m_n/m_0$, and in matrix notation

$$P(\omega) = (m_0\omega^2 - \Phi)^{-1} \tag{3b}$$

is the Green's function for the perfect host lattice of atoms of mass m_0. The imaginary part of $G(l, l'; \omega)$ gives the displacement-displacement correlation function

$$\langle u_\alpha(l) u_\beta(l')\rangle_\omega = (\hbar/\pi)(e^{-\hbar\beta\omega} - 1)^{-1} \mathrm{Im} G_{\alpha\beta}(l, l'; \omega) . \tag{4}$$

We evaluate the thermal-conductivity tensor for a cubic crystal, where after configuration averaging one finds $\langle \kappa_{\alpha\beta}\rangle = \kappa\delta_{\alpha\beta}$ via the Kubo formula[15]

$$\kappa(q=0,\ \omega)=\lim_{\eta\to 0}(L^dT)^{-1}\int_0^\infty dt\, e^{-\eta t}e^{i\omega t}\times\int_0^\infty d\lambda\,\langle S_\alpha(q=0,\ 0)S_\alpha(q=0,\ t+i\hbar\lambda)\rangle_T\ , \quad (5)$$

where L^d is the d-dimensional size of the system, η is the adiabatic switching parameter, and $\vec{S}$ is the thermal-current-density operator, which is related to the local energy-density operator through the continuity equation

$$\dot{\mathcal{H}}(x)+\nabla\cdot\vec{S}(x)=0\ . \quad (6)$$

By expressing the thermal average $\langle\ldots\rangle_T$ in terms of the trace over the exact eigenstates $\{n\}$ of the system, with energy $\{\epsilon_n\}$, the time and temperature integrals of Eq. (5) can be performed, with the result

$$\kappa(\omega)=-i\hbar(L^dT)^{-1}\sum_{n,n'}(\hbar\omega+i\eta+\epsilon_{n'}+\epsilon_n)^{-1}(\epsilon_{n'}-\epsilon_n)^{-1}\times(1-e^{\beta(\epsilon_{n'}-\epsilon_n)})\langle n|S_\alpha|n'\rangle Z^{-1}e^{-\beta\epsilon_{n'}}\langle n'|S_\alpha|n\rangle\ , \quad (7)$$

where Z is the partition function. For the dc conductivity ($\omega=0$) this result can be written

$$\kappa=-i\hbar(L^dT)^{-1}\int_{-\infty}^{\infty}(\epsilon+i\eta)^{-1}\epsilon^{-1}(1-e^{\beta\epsilon})J(\epsilon)\,d\epsilon\ , \quad (8)$$

where

$$J(\epsilon)=\sum_{n,n'}\langle n|S_\alpha|n'\rangle Z^{-1}e^{-\beta\epsilon_{n'}}\langle n'|S_\alpha|n\rangle\times\delta(\epsilon-(\epsilon_{n'}-\epsilon_n))\ . \quad (9)$$

The Kubo form for the thermal conductivity is obtained by first separating Eq. (8) into its real and imaginary parts and then noting [from Eq. (9)] that

$$J(-\epsilon)=e^{\beta\epsilon}J(\epsilon)\ , \quad (10)$$

so that the imaginary part of Eq. (8) vanishes. This leaves only the real part of Eq. (8), which takes the form

$$\kappa=\pi\hbar\beta\frac{J(0)}{(L^dT)}\ . \quad (11)$$

We evaluate $J(0)$ by calculating the Fourier components of the retarded current-current Green's function, which are related to J by[11]

$$\mathrm{Im}\langle\langle S_\alpha;\ S_\alpha\rangle\rangle_\omega=-\pi(e^{\hbar\beta\omega}-1)J(\hbar\omega)\ , \quad (12)$$

or

$$J(0)=-(\pi\hbar\beta)^{-1}\left.\frac{d(\mathrm{Im}\langle\langle S_\alpha;\ S_\alpha\rangle\rangle_\omega)}{d\omega}\right|_{\omega=0}\ . \quad (13)$$

To proceed further, we use the harmonic form of the thermal-current-density operator $\vec{S}$ evaluated by Hardy.[10] In this form Hardy included the kinetic and potential energy densities and solved Eq. (6) for $\vec{S}$, neglecting all terms not quadratic in displacement and momentum operators (including those coming from the anharmonic part of the Hamiltonian). This result is

$$\vec{S}(q=0)=\frac{1}{2}\sum_{ll',\alpha\beta}(\vec{x}_l-\vec{x}_{l'})\phi_{\alpha\beta}(l,\ l')v_\alpha(l)u_\beta(l')=\sum_{ll',\alpha\beta}\vec{A}_{\alpha\beta}(l,\ l')v_\alpha(l)u_\beta(l')\ , \quad (14)$$

where $v_\alpha(l)=p_\alpha(l)/m_l$ is the velocity of the lth atom in the αth direction. Therefore, to evaluate Eq. (13), we calculate the two-phonon Green's function $\langle\langle v(1,\ t)u(2,\ t);\ v(3,\ 0)u(4,\ 0)\rangle\rangle$. This retarded Green's function can always be expanded exactly to the form

$$\langle\langle v(1,\ t)u(2,\ t);\ v(3,\ 0)u(4,\ 0)\rangle\rangle=(i\hbar)^{-1}\theta(t)\,\langle v(1,\ t)[u(2,\ t),\ v(3,\ 0)]\,u(4,\ 0)+v(1,\ t)v(3,\ 0)[u(2,\ t),\ u(4,\ 0)]+[v(1,\ t),\ v(3,\ 0)]u(4,\ 0)u(2,\ t)+v(3,\ 0)[v(1,\ t),\ u(4,\ 0)]u(2,\ t)\rangle_T\ , \quad (15)$$

where $v(1,\ t)$ is a simpler notation for $v_\alpha(l,\ t)$. Since we have assumed the harmonic approximation, moreover, these four-operator averages decouple exactly into pairs of two-operator averages, because the commutators in (15) are c numbers. This factoring results, when Fourier transformed, in the four convolutions

$$\langle\langle\vec{S};\ \vec{S}\rangle\rangle_z=\sum_{1,2,3,4}\vec{A}(1,\ 2)\vec{A}(3,\ 4)\int_{-\infty}^{\infty}d\omega[\langle v(1)u(4)\rangle_\omega\langle\langle u(2);\ v(3)\rangle\rangle_{z-\omega}+\langle v(1)v(3)\rangle_\omega\langle\langle u(2);\ u(4)\rangle\rangle_{z-\omega}+\langle u(4)u(2)\rangle_{-\omega}\langle\langle v(1);\ v(3)\rangle\rangle_{z-\omega}+\langle v(3)u(2)\rangle_{-\omega}\langle\langle v(1);\ u(4)\rangle\rangle_{z-\omega}]\ , \quad (16)$$

where $\langle vu\rangle_\omega$ and $\langle\langle v;\ u\rangle\rangle_\omega$ are the Fourier components of $\langle v(t)u(0)\rangle_T$ and $\langle\langle v(t);\ u(0)\rangle\rangle$, respectively. These four terms can now be collected together. Using the definition of the remaining double-time Green's functions analogous to Eq. (2), the following identities may easily be established by examining the resulting equations of motion and comparing with that for $G(\omega)$; we find

$$\langle\langle v(l);\ v(l')\rangle\rangle_\omega=-m_l^{-1}\delta_{ll'}+\omega^2G(l,\ l';\ \omega)\ , \quad (17a)$$

$$\langle\langle v(l);\ u(l')\rangle\rangle_\omega=-i\omega G(l,\ l';\ \omega)\ , \quad (17b)$$

and

$$\langle\langle u(l);\ v(l')\rangle\rangle_\omega=i\omega G(l,\ l';\ \omega)\ . \quad (17c)$$

Similarly, the corresponding correlation functions

are related to their Green's functions as in Eq. (4), which gives

$$\langle v(l)\,v(l')\rangle_\omega = (\hbar/\pi)\,\omega^2 f(-\omega)\,\mathrm{Im}G(l,\,l';\,\omega) \quad (18a)$$

and

$$\langle v(l)\,u(l')\rangle_\omega = (\hbar/\pi)\,i\omega f(-\omega)\,\mathrm{Im}G(l,\,l';\,\omega)\,, \quad (18b)$$

where $f(\omega)=(e^{\hbar\beta\omega}-1)^{-1}$ is the Planck distribution function. If we then make the indicated substitutions back into Eq. (16), we find

$$\langle\langle \vec{S};\,\vec{S}\rangle\rangle_z = \frac{\hbar}{\pi}\sum_{1,2,3,4} A(1,\,2)A(3,\,4)\int_{-\infty}^{\infty} d\omega\{\omega(z-\omega)f(-\omega)\,\mathrm{Im}G(1,\,4,\,\omega)\,G(2,\,3;\,z-\omega)$$

$$+\omega^2 f(-\omega)\,\mathrm{Im}\,G(1,\,3,\,\omega)G(2,\,4;\,z-\omega) - f(\omega)\,\mathrm{Im}G(3,\,4,\,\omega)[-m_1^{-1}\delta_{13}+(z-\omega)^2 G(1,\,3;z-\omega)]$$

$$-\omega(z-\omega)f(\omega)\,\mathrm{Im}G(2,\,3,\,\omega)G(1,\,4;\,z-\omega)\}\,, \quad (19)$$

where the easily derived general symmetry with respect to complex conjugation,

$$G(l,\,l';\,-z)=G^*(l',\,l;\,z)\,, \quad (20)$$

has been used to handle the negative-frequency correlations. We, however, according to the energy current formula (13), only need evaluate the derivative of the imaginary part of Eq. (19) at zero frequency, $z=0$. This quantity, with the use of the antisymmetry $\vec{A}(1,\,2)=-\vec{A}(2,\,1)$ as inferred from Eq. (14), simplifies Eq. (19) considerably as the terms collect together to give

$$\frac{d}{dz}\,\mathrm{Im}\langle\langle \vec{S};\,\vec{S}\rangle\rangle_z\big|_{z=0} = \frac{\hbar}{\pi}\int_{-\infty}^{\infty} d\omega\Big[-\frac{\omega(e^{\beta\hbar\omega}+3)}{e^{\beta\hbar\omega}-1}$$

$$\times\mathrm{Tr}\{\mathrm{Im}[G(\omega)]A\,\mathrm{Im}[G(\omega)]A\}$$

$$+\,2\omega^2\,\frac{e^{\beta\hbar\omega}+1}{e^{\beta\hbar\omega}-1}\,\mathrm{Tr}\Big(A\,\mathrm{Im}[G(\omega)]A\,\frac{d}{d\omega}\,\mathrm{Im}[G(\omega)]\Big)\Big]\,, \quad (21)$$

where in the last term the relation

$$\frac{d}{dz}\,\mathrm{Im}G(l,\,l',\,z-\omega)\big|_{z=0} = \frac{d}{d\omega}\,\mathrm{Im}G(l',\,l,\,\omega)\,, \quad (22)$$

which follows immediately from Eq. (20), has been used. Now, by the cyclic symmetry of the trace, we note that

$$\mathrm{Tr}\Big(A\,\mathrm{Im}[G(\omega)]A\frac{d}{d\omega}\,\mathrm{Im}[G(\omega)]\Big)$$

$$=\frac{1}{2}\frac{d}{d\omega}\,\mathrm{Tr}\{A\,\mathrm{Im}[G(\omega)]A\,\mathrm{Im}[G(\omega)]\}\,, \quad (23)$$

so that, after an integration of the last term in Eq. (21) by parts, we find that Eq. (21) becomes

$$\frac{d}{dz}\,\mathrm{Im}\langle\langle \vec{S};\,\vec{S}\rangle\rangle_z\big|_{z=0} = \frac{2\beta\hbar^2}{\pi}\int_{-\infty}^{\infty} d\omega\,\frac{\omega^2 e^{\beta\hbar\omega}}{(e^{\beta\hbar\omega}-1)^2}$$

$$\times\,\mathrm{Tr}\{A\,\mathrm{Im}[G(\omega)]A\,\mathrm{Im}[G(\omega)]\}\,. \quad (24)$$

Thus the dc thermal conductivity (11) is

$$\kappa = \frac{2\hbar^2\beta}{\pi L^4 T}\int_{-\infty}^{\infty} d\omega\,\frac{\omega^2 e^{\beta\hbar\omega}}{(e^{\hbar\beta\omega}-1)^2}$$

$$\times\,\mathrm{Tr}\{A\,\mathrm{Im}[G(\omega)]A\,\mathrm{Im}[G(\omega)]\}\,. \quad (25)$$

III. APPLICATION TO DISORDERED SYSTEMS

The discussion and results of the last section would apply to any particular system of masses and force constants providing only that the forces are harmonic and the displacements of the atoms from the regular lattice sites are small. This assumption was necessary to allow the decoupling of the two-phonon Green's function in Eq. (16), and to neglect the higher-order terms in the energy current operator as in the derivation of formula (14).

We now wish, for simplicity, to limit our calculation to the simple model of an isotopic, binary alloy where the force constants $\phi_{\alpha\beta}(l,\,l')$ in Eq. (1) are assumed to be the same regardless of the types of atoms on the sites and where the only configuration-dependent term in the Hamiltonian is the mass m_l of the atom at each site l. For a single impurity mass (or only a few impurity masses) in an otherwise perfect, infinite chain, the physical properties can be calculated exactly. But for finite concentrations of impurities the exact calculation becomes hopeless and analytic progress can be made only by the taking of an ensemble average over all configurations of the impurities on the lattice.

First we consider the configuration average of the one-phonon Green's function $\langle G\rangle$ within the coherent-potential approximation to set the notation. Iterating Eq. (3) gives

$$G_{\alpha\beta}(l,\,l';\,\omega) = P_{\alpha\beta}(l,\,l';\,\omega) + \sum_{n,\gamma} P_{\alpha\gamma}(l,\,n,\,\omega)\,V_n P_{\gamma\beta}(n,\,l';\,\omega)$$

$$+\sum_{n,m,\gamma,\delta} P_{\alpha\gamma}(l,n;\omega)V_nP_{\gamma\delta}(n,m;\omega)V_mP_{\delta\beta}(m,l',\omega)+\cdots . \quad (26)$$

This equation can be exactly rewritten by collecting together all successive scattering by the same site to form the equation

$$G(l,l')=P(l,l')+\sum_n P(l,n)t_n'P(n,l')+\sum_{n\neq m} P(l,n)t_n'P(n,m)t_m'P(m,l') + \sum_{n\neq m\neq r} P(l,n)t_n'P(n,m)t_m'P(m,r)t_r'P(r,l')+\cdots . \quad (27)$$

where the Cartesian indices have been absorbed into the site index and where the single-site t matrix

$$t_n' = \frac{V_n}{1-V_nP(n,n;\omega)} \quad (28)$$

includes all successive scatterings by site n.

The essence of the coherent-potential approximation (CPA) is to assume that the unperturbed propagator P is modified to include a self-energy Σ (or coherent potential as it is called in the electronic calculation) or that P is replaced by

$$G^0 = P(1-\Sigma P)^{-1} . \quad (29)$$

In terms of the new unperturbed propagator, Eq. (27) becomes, after rearrangement and configuration averaging,

$$\langle G(l,l)\rangle = G^0(l,l')+\sum_n G^0(l,n)\langle t_n\rangle G^0(n,l') + \sum_{n\neq m} G^0(l,n)\langle t_nG^0(n,m)t_m\rangle G^0(m,l')+\cdots , \quad (30a)$$

where the single-site t matrix is

$$t_n = \frac{V_n-\Sigma}{1-(V_n-\Sigma)G^0(n,n;\omega)} , \quad (30b)$$

since $V_n-\Sigma$ is the new perturbation relative to G^0. If the self-energy Σ were the true self-energy, than G^0 would be $\langle G\rangle$, or the second and higher terms in Eq. (30a) would be zero. The best approximation with a site-diagonal self-energy $\Sigma_{nm} = \delta_{nm}\Sigma$ is that obtained by setting the average single site t matrix $\langle t_n\rangle$ to zero;

$$\langle t_n\rangle = \frac{(1-c)(V_A-\Sigma)}{1-(V_A-\Sigma)G^0(n,n)} + \frac{c(V_B-\Sigma)}{1-(V_B-\Sigma)G^0(n,n)} = 0 , \quad (31)$$

and neglecting all higher nonzero terms in Eq. (30). Such a calculation has been made and discussed by several authors and is equivalent to the self-consistent single-site-scattering diagrammatic approach. For our calculation, we choose $m_0 = m_A$, or the A-atom lattice is the unperturbed lattice, so that

$$V_A = 0, \quad V_B = m_A\epsilon_B\omega^2 = (m_A-m_B)\omega^2 , \quad (32)$$

so that Eq. (32) simplifies to the equation

$$\frac{(1-c)\Sigma}{1+\Sigma G^0(n,n)} = \frac{c(V_B-\Sigma)}{1-(V_B-\Sigma)G^0(n,n)} , \quad (33a)$$

or

$$\Sigma = \frac{cV_B}{1-(V_B-\Sigma)G^0(n,n)} , \quad (33b)$$

which must be solved simultaneously with Eq. (29) to find G^0. As has been discussed previously, the value G^0 obtained from Eqs. (29) and (31) is independent of the unperturbed mass m_0 so that the formula can equally be viewed as a perturbation formula about $m_0=m_A$, the A-atom lattice, $m_0=m_B$, the B-atom lattice, or $m_0=\langle m\rangle$, the virtual or mean crystal. Thus the formula is an interpolation formula of use at all concentrations.

However, our main purpose here was to calculate the average thermal conductivity which, from Eq. (25) requires knowledge of the average of

$$\mathrm{Tr}\langle A\,\mathrm{Im}[G(\omega)]A\,\mathrm{Im}[G(\omega)]\rangle = \tfrac{1}{4}\mathrm{Tr}\langle A[G(\omega)-G^*(\omega)]A[G^*(\omega)-G(\omega)]\rangle . \quad (34a)$$

where $G^*(\omega)$ is the complex conjugate or advanced Green's function. This requires averages of two Green's functions such as

$$\mathrm{Tr}\langle AG(\omega)AG^*(\omega)\rangle . \quad (34b)$$

The expansion of $G(\omega)$ in terms of $G^0(\omega)$ according to Eq. (30), but before averaging, yields

$$\sum_l \langle A(l,n)G(n,m)A(m,p)G(p,l)\rangle = \sum_l \Big\langle A(l,n)\Big(G^0(n,m)+\sum_1 G^0(n,1)t_1G^0(1,m) + \sum_{1\neq 2} G^0(n,1)t_1G^0(n,1)t_1G^0(1,2)t_2G^0(2,m)+\cdots\Big)A(m,p) \times\Big(G^0(p,l)+\sum_{1'}G^0(p,1')t_{1'}G^0(1',l)+\sum_{1'\neq 2'}G^0(n,1')t_{1'}G^0(1',2')t_{2'}G^0(2',l)+\cdots\Big)\Big\rangle , \quad (35)$$

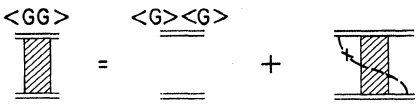

FIG. 1. Diagrams appearing in the expansion of the two-particle Green's function within the CPA, where the dashed line represents the t matrix for all successive scatterings of the two phonons off a lattice point.

where G^0 is the solution of Eqs. (29) and (31), and where the average of a single $\langle t\rangle$ is zero. Thus, in the spirit of the CPA, and consistent with the appropriate Ward identity, only terms with an even number of t's are assumed to survive the average in (35) and then only the average $\langle t_n^2\rangle$ is kept, so that averages decouple in a nested fashion:

$$\langle t_1 t_2 t_3 \cdots t_{n-2} t_{n-1} t_n\rangle \cong \langle t_1 \langle t_2 \langle t_3 \langle \cdots\rangle t_{n-2}\rangle t_{n-1}\rangle t_n\rangle = \langle t_n^2\rangle^{n/2} \delta_{1,n}\delta_{2,n-1}\delta_{3,n-2}\cdots . \tag{36}$$

This is equivalent to having summed the diagrams shown in Fig. 1 for $\langle GG\rangle$. When this decoupling is sandwiched with the A's in Eq. (35), there is left, as the middle term in the average, a quantity of the form

$$\sum_m G^0(n, m) A(m, p) G^{0*}(p, n) , \tag{37}$$

since the last scattering from the left-hand G must be by the same site n as the first scattering on the right-hand G. But the quantity in Eq. (37) is zero in any crystal with inversion symmetry, since then G^0 would be even under inversion and A, because of the $\vec{x}_l - \vec{x}_{l'}$ in Eq. (14), is odd. Thus all of the vertex corrections in the CPA contribute nothing to the thermal conductivity and the average factors into $\mathrm{Tr}[A\langle G\rangle A\langle G^*\rangle]$. The argument follows likewise for the other terms in (35a), so that the average conductivity from Eq. (25) becomes

$$\langle\kappa\rangle \cong -\frac{2\hbar^2\beta}{\pi L^d T}\int_{-\infty}^{\infty} d\omega\, \frac{\omega^2 e^{\beta\hbar\omega}}{(e^{\hbar\beta\omega}-1)^2} \times \mathrm{Tr}[A\langle \mathrm{Im}G^0(\omega)\rangle A\langle \mathrm{Im}G^0(\omega)\rangle] . \tag{38}$$

This result holds because the isotopic defects and the CPA allow only s-wave scattering; whenever either extended defects or pair or higher scattering is included, the vertex corrections contribute. This formula reduces to that of Woll[6] for low concentrations.

The evaluation of $\langle\kappa\rangle$ would seem routine; now that $G^0(\omega)$ is known, Eq. (38) is simply evaluated. However, there is an infrared divergence in Eq. (38) which must be handled before a numerical calculation can proceed. This low-frequency divergence appears in systems of arbitrary dimension regardless of the disorder.

The trace in formula (38) can be carried out in k representation,

$$\mathrm{Tr}\{A\,\mathrm{Im}[G(\omega)]A\,\mathrm{Im}[G(\omega)]\} = \frac{1}{N}\sum_k A_{(k)}^2 [\mathrm{Im}G(\vec{k}, \omega)]^2 , \tag{39}$$

since G^0 has the lattice symmetry, where the $\vec{k}$ index includes any polarization mode indices, and where, from Eqs. (3b), (14), and (29),

$$G(k, \omega) = [m_0\omega^2 - m_0\omega_{\vec{k}}^2 - \mathrm{Re}\Sigma(\omega) - i\,\mathrm{Im}\Sigma(\omega)]^{-1} \tag{40a}$$

and

$$A(k) = im_0\omega_{\vec{k}}^* v_{\vec{k}}^* \sim im_0 v_s \omega_{\vec{k}}^* \quad \text{for small } \vec{k}, \tag{40b}$$

with v_s being the speed of sound. To sort out the nature of the infrared divergence we shall study the low-frequency ω limit, which in turn means that the contribution to the sum in (39) will occur at small k. Hence, to evaluate Eq. (39) we need

$$\frac{1}{N}\sum_{\vec{k}} (v_s\omega_{\vec{k}})^2 \{\mathrm{Im}[(\omega^2 - \omega_{\vec{k}}^2 - \mathrm{Re}\Sigma - i\,\mathrm{Im}\Sigma)^{-1}]\}^2 \underset{N\to\infty}{\sim} \alpha\int_{-\infty}^{\infty} \frac{d\omega'\omega'^2\rho(\omega')[\mathrm{Im}\Sigma(\omega)]^2}{\{[m_0\omega^2 - m_0\omega'^2 - \mathrm{Re}\Sigma(\omega)]^2 + [\mathrm{Im}\Sigma(\omega)]^2\}^2} , \tag{41}$$

where $\rho(\omega')$ is the perfect-lattice density of states. For small ω, the imaginary part of the self-energy from Eq. (33b) is also small, namely,

$$\mathrm{Im}\Sigma(\omega) \sim c\, v_B^2\, \mathrm{Im}G^0(\omega) \sim \alpha\omega^4\omega^{d-2} \quad \text{for small } \omega, \tag{42}$$

where d is the dimensionality of the system; this property is general in that the lifetime of phonons due to disorder scatterings diverges as $\tau \sim \omega^{-(d+2)}$ at low frequencies. The long-wavelength phonons do not see the disorder.

In the contour integration of (41) about either complex ω' half-plane, two of the four poles of the integrand at

$$\omega' = \pm[\omega^2 - \mathrm{Re}\Sigma(\omega)m_0 \pm i\,\mathrm{Im}\Sigma(\omega)m_0]^{1/2} \tag{43}$$

contribute. From the vanishing of $\mathrm{Im}\Sigma(\omega)$ as $\omega \to 0$, one can easily see that the divergent contribution to the residues gives

$$\mathrm{Tr}\{A\,\mathrm{Im}[G(\omega)]A\,\mathrm{Im}[G(\omega)]\} \underset{\omega\to 0}{\sim} \frac{\omega\rho(\omega)}{\mathrm{Im}\Sigma(\omega)} , \tag{44}$$

so that the integrand of the conductivity formula (38) becomes proportional to

$$\frac{\omega^3 e^{\beta\hbar\omega}\rho(\omega)}{(e^{\hbar\beta\omega}-1)^2\,\mathrm{Im}\Sigma(\omega)} \underset{\omega\to 0}{\sim} \frac{\omega^3\omega^{d-1}}{\omega^2\omega^{d+2}} = \frac{1}{\omega^2} \tag{45}$$

regardless of the dimension of the system, where the limiting behavior followed from Eq. (42). Thus there is a nonintegrable $1/\omega^2$ divergence in the integrand (38) at $\omega = 0$. This divergence is due to the fact that the long-wavelength phonons are not

scattered by the disorder and because they move at the speed of sound. A similar divergence does not appear in the corresponding electrical conductivity problem,[14] since low-frequency electrons move slowly. [The vanishing $v_{\vec{k}}$ in $A(\vec{k})$ kills the divergence.]

The existence of this divergence is clearly physical; it is removed in real systems by other phonon scattering mechanisms, such as boundary scattering or anharmonic phonon interactions. The effect of these other mechanisms (at low concentrations) has been discussed extensively in the literature.[9] For the purposes of providing some insight into the concentration effects by doing a numerical calculation, we limit the divergence somewhat artificially in two ways. First, we follow the approach of Woll[6] and limit our calculations to a finite sample by cutting off the integral (38) at a low frequency,

$$\omega_{\min} = \frac{V_s \pi}{Na} \quad , \tag{46}$$

the minimum nonzero frequency for a system with periodic boundary conditions of the linear dimension $L = Na$, where N is the number of atoms along this length separated by a lattice spacing a. The cutoff in the integral of $1/\omega^2$ produces, for large N, a result

$$\kappa \sim \int_{\omega_{\min}} \frac{d\omega}{\omega^2} \sim \alpha\, \omega_{\min}^{-1} = \frac{\alpha a N}{\pi V_s} \, , \tag{47}$$

so that for a linear chain the thermal conductivity diverges linearly with N, the number of atoms in the chain. This result differs from that of other approaches[2-4,16] where an $N^{1/2}$ divergence is found. We can only speculate at this point that perhaps the exponent depends strongly upon the boundary conditions of the chain. Calculations of κ with this cutoff are presented in Sec. IV for one-, two-, and three-dimensional systems.

Second, for a three-dimensional system, we add empirically an umklapp anharmonic phonon scattering term, via a Matheissen's rule, to ascertain some of the effect of anharmonicity,

$$\frac{1}{\tau_{\text{tot}}(\omega)} = \frac{1}{\tau_{\text{dis}}(\omega)} + \frac{1}{\tau_{\text{umk}}(\omega)} \quad . \tag{48}$$

This addition, when included in the self-energy, gives

$$\text{Im}\Sigma_T(\omega) = \text{Im}\Sigma(\omega) + \frac{\omega}{\tau(\omega)} \quad , \tag{49}$$

where $\tau(\omega)$ is chosen to be the low-frequency high-temperature form

$$\tau(\omega) = \lambda/\omega^2 \, . \tag{50}$$

For three-dimensional systems $\text{Im}\Sigma_T(\omega)$ now vanishes only as ω^3, rather than the ω^5 in Eq. (42) and the divergence is removed.

IV. NUMERICAL RESULTS

In this section we show the result of calculation of formula (38) for one-, two-, and three-dimensional systems. These results are compared with those from the computer experiments of Payton *et al.*

Since the self-energy $\Sigma_{\text{CPA}}(\omega)$ is independent of $\vec{k}$, it is easily seen that

$$G_{\text{CPA}}(\omega) = P(\omega[1 - \Sigma_{\text{CPA}}(\omega)/m_0\omega^2]^{1/2}) \, , \tag{51}$$

or the alloy Green's function on the real ω axis is the perfect lattice Green's function evaluated at a complex frequency $z = \omega(1 - \Sigma/m_0\omega^2)^{1/2}$. This equation must be solved simultaneously with the CPA equation (33b) to obtain G_{CPA}.

A. One Dimension

For a perfect, harmonic, linear chain with only nearest-neighbor forces, the diagonal part of the one-phonon Green's function is

$$P(0,\, 0;\, \omega + i\epsilon) = \frac{1}{m_0\, \omega(\omega^2 - \omega_0^2)^{1/2}} \, , \tag{52}$$

where $\omega_0^2 = 4\phi/m_0$ is the maximum phonon frequency of the perfect lattice. The simultaneous solution of Eqs. (33b), (51), and (52) was then easily done using Wegstein's iteration method[17] generalized to a function of a complex variable which converged very rapidly (in less than ten iterations in all cases) provided we began at low frequencies using $\Sigma(\omega) = cm_0\epsilon\omega^2$ as the first guess.

The trace in Eq. (39) was evaluated in reciprocal space, where it takes the form

$$\text{Tr}(A\langle \text{Im}G\rangle A\,\langle \text{Im}G\rangle) = \sum_{\vec{k}} \frac{v_{\vec{k}}^2\, \omega_{\vec{k}}^2}{[m_0\omega^2 - m_0\omega_{\vec{k}}^2 - \text{Re}\Sigma(\omega) - i\,\text{Im}\Sigma(\omega)]^2} \, . \tag{53}$$

With a sufficiently small grid size this formula was approximated, within each cell, as

$$\sum_{\vec{k}} \frac{v_{\vec{k}}^2\, \omega_{\vec{k}}^2}{[m_0\omega^2 - m_0\omega_{\vec{k}_0}^2 - 2\omega_{\vec{k}_0} m_0 \nabla\omega_{\vec{k}} \cdot \vec{k} - \text{Re}\Sigma(\omega) - i\,\text{Im}\Sigma(\omega)]^2} \, , \tag{54}$$

where $\omega_{\vec{k}_0}$ is the value of $\omega_{\vec{k}}$ at the center of that cell. This integral was then carried out analytically within the cell. This procedure is that of Gilat and Raubenheimer.[18] The size of the grid was taken to be $0.01\pi/a$ in the calculation here.

The final frequency integration was done using

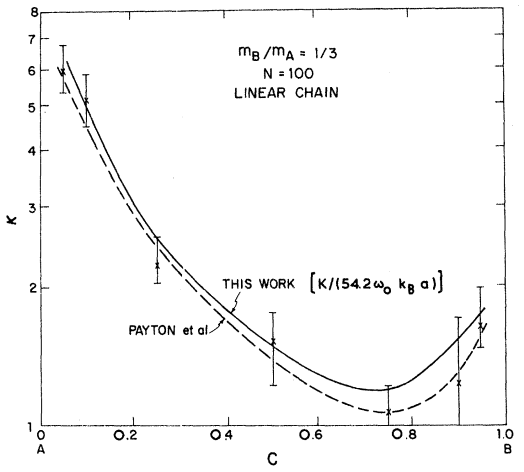

FIG. 2. Thermal conductivity of a harmonic linear chain of 100 atoms as given by Eq. (38) versus concentration of B atoms (solid line) in units of $54.2\omega_0 k_B a$, and the computer experimental results of Ref. 1 (dashed line) in their units.

Simpson's rule with intervals of $0.01\omega_0$ where, because of the infrared divergence, the integral was cut off at low frequencies at $\omega_{\min}$, the lowest-frequency phonon in the chain of N atoms as discussed in Sec. III. The infrared divergence could also have been removed by adding an empirical boundary scattering term to the self-energy which presumably would have given similar results.

The numerical results are shown in Fig. 2 for a disordered chain with $m_B = \frac{1}{3}m_0$ and $N = 100$ in the high-temperature limit. The results are plotted versus concentration from 0 to 100% and compared with the computer experiments of Payton *et al.*,[1] which had precisely the same Hamiltonian and were also for a 100-atom chain. The qualitative agreement with the concentration dependence is reasonably good. The thermal conductivity for this work is plotted in units of $54.2\omega_0 k_B a$. This choice of units was chosen to fit the over-all magnitude of this calculation to that of Ref. 1 on the graph in that reference. The formula given in Ref. 1 for conversion of their result to mks units differs from this work so that this calculation is larger than theirs by an unexplained factor of 10.8 for $N = 100$. This difference could conceivably be real, coming from the different choice of boundary conditions in this peculiar system.

The principal qualitative feature common to both curves of κ is the asymmetry about $c = 0.5$. This asymmetry, which reduces the conductivity for small concentration of the heavy atoms, must be due to the presence of low-frequency in-band resonant impurity modes which, due to the low-frequency weighting, is especially effective at reducing heat flow. In this CPA calculation this effect is produced by different shapes of the density-of-states curve when there are low-frequency resonant modes. A higher-order calculation, with nonvanishing vertex contributions, should show that these modes actually are fairly localized in space and hence that the thermal conductivity is reduced even more than that given by the density-of-states effect here and hence that the curve is more asymmetric than this CPA calculation indicates.

B. Two and Three Dimensions

In higher-dimensional systems there does not exist such a simple analytic form for the perfect-lattice frequency spectrum or Green's function. Nevertheless, the frequency spectrum is known numerically either from various experiments or, as in this case, from a model dynamical matrix calculation. Therefore the analytic continuation (51) of the perfect-lattice frequency spectrum $\rho(\omega)$ to the complex frequency plane is carried out numerically by the integral transform

$$G_{\mathrm{CPA}}(\omega) = \frac{1}{\pi m_0}\int_0^\infty \frac{\rho(\omega')\,d\omega'}{\omega^2 - \omega'^2 - \Sigma_{\mathrm{CPA}}(\omega)/m_0} \quad . \tag{55}$$

The frequency spectra used in the calculations here were determined by diagonalization of the appropriate dynamical matrices with only nearest-neighbor forces on a grid of points within the irreducible part of the Brillouin zone using the numerical integration method of Gilat and Raubenheimer.[18] Our resulting frequency spectrum $\rho(\omega)$ is shown, for illustration, in Fig. 3 for the fcc structure.

The thermal-conductivity results, Eq. (38), for a simple square lattice in the high-temperature

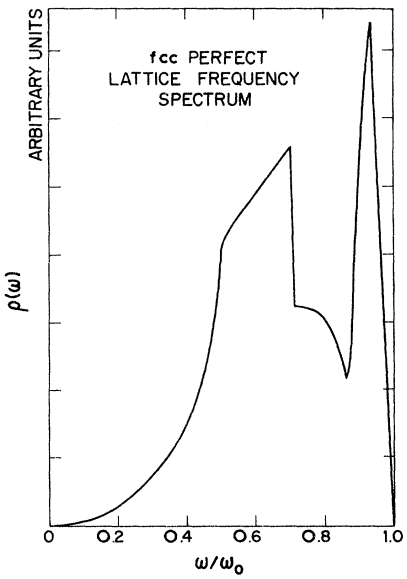

FIG. 3. Phonon frequency spectrum of a fcc perfect lattice with nearest-neighbor forces.

limit are shown versus concentration in Fig. 4 for a 100×100-atom sample. These results (solid line) are plotted in units of $27.1\omega_0 k_B$ and are compared with the results of Payton *et al.* (dashed curve) in their units. These results are larger in over-all magnitude than those of Ref. 1 by a factor of about 5.4.

The concentration dependence, while asymmetric about $c = 0.5$, is less asymmetric than that of computer experiments. It should be pointed out that this asymmetry is a function of the size of the sample chosen; a larger N leads to less asymmetry. This behavior follows from the infrared divergence in the integral (38). When the low-frequency cutoff $\omega_{\min}$ is small (large N), the very-low-frequency modes dominate and these long-wavelength modes are less affected by impurity scattering. The point here is that if the mean free path of phonons is very long (due to boundary scattering, phonon-phonon-phonon scattering, etc.) for the long-wavelength phonons which do not see the disorder, then these modes dominate the heat transport. Calculations were performed for $N = 2000$ and showed a quite symmetric curve.

Qualitatively similar results were obtained for a three-dimensional fcc lattice alloy in the high-temperature limit. These results are shown in Fig. 5(a) for a simple 100 atoms in linear dimension, where κ is plotted in units of $27.1\omega_0 k_B/a$ for comparison with the other graphs. Unfortunately, no computer experiments exist for comparison for the fcc lattice.

In real systems at high-temperature, phonon-phonon umklapp scattering is the dominant scattering mechanism. This scattering will also remove

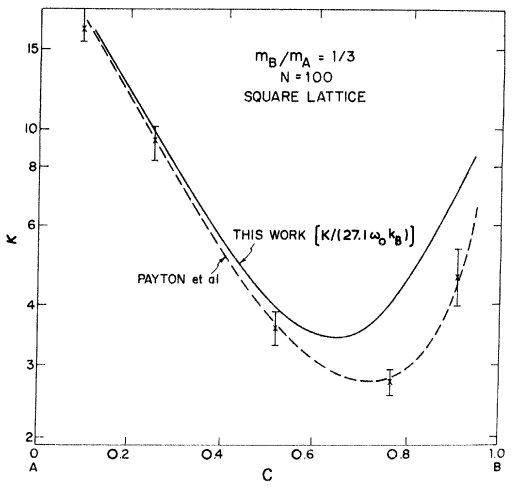

FIG. 4. Thermal conductivity of a 100× 100-atom, harmonic, simple square lattice as given by Eq. (38) versus concentration of B atoms (solid line) in units of $27.1\omega_0 k_B$, and the computer experimental results of Ref. 1 (dashed line) in their units.

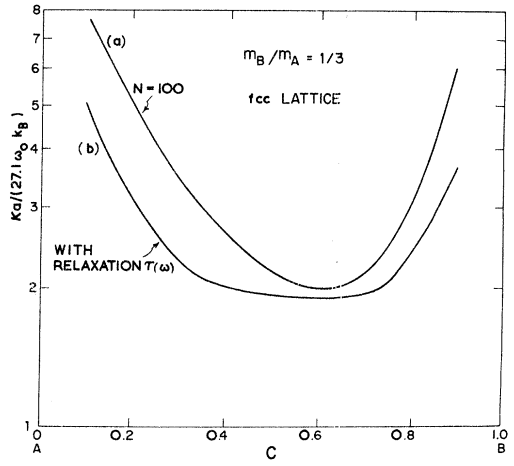

FIG. 5. (a) Thermal conductivity of a 100 × 100 × 100-atom, harmonic fcc lattice as given by Eq. (38) versus concentration of B atoms; (b) thermal conductivity of a fcc lattice with the modification of an extra scattering term (50) like that from umklapp phonon-phonon scattering.

the infrared divergence.[9] In Fig. 5(b), we plot the results of additively including an extra scattering time $\tau(\omega)$, given by Eq. (50), where λ was chosen so that the extra scattering term $\Sigma_{\text{umk}}(\omega)$ was as large as $\Sigma_{\text{CPA}}(\omega)$ at the previous cutoff $\omega_{\min}$ ($N = 100$). The effect of this anharmonicity is to flatten and thus make more symmetric the thermal-conductivity curve.

V. CONCLUSIONS

We have developed a formalism for calculating the thermal conductivity of a high-concentration alloy in the harmonic approximation (the impurity resistance). Comparisons with computer experiments performed within the same model show reasonable agreement with the concentration dependence but give a conductivity smaller in over-all magnitude than that calculated here within the CPA (by a factor of about 10.8 and 5.4 in the one- and two-dimensional cases, respectively).

A most interesting challenge remaining in this problem is to calculate the effect of adding anharmonicity to the model where Payton *et al.* have observed an increase rather than a decrease, in the thermal conductivity in their simple systems. This increase would seem to be due to the allowance of an extra mechanism whereby localized-state phonons, which were unable to participate in the conduction in the harmonic model, can hop from localized state to localized state via virtual decay into two- or more-band phonons when anharmonicity is added.

ACKNOWLEDGMENTS

We should like to acknowledge useful comments from Dr. D. N. Payton and Dr. W. M. Visscher.

*Supported in part by the National Science Foundation. This work will constitute part of a Ph. D. thesis to be submitted by J. K. F. to Rutgers University.

[1]D. N. Payton, M. Rich, and W. M. Visscher, Phys. Rev. 160, 706 (1967).

[2]A. Casher and J. L. Liebowitz, J. Math. Phys. 12, 1701 (1971).

[3]H. Matsuda and K. Ishii, Prog. Theor. Phys. Suppl. (Kyoto) 45, 56 (1970).

[4]R. J. Rubin and W. L. Greer, J. Math. Phys. 12, 1686 (1971); W. L. Greer and R. J. Rubin, J. Math. Phys. 13, 379 (1972).

[5]See, for example, the footnote on p. 732 in the paper by W. M. Visscher [Progr. Theoret. Phys. (Kyoto) 46, 729 (1971)].

[6]E. J. Woll, Phys. Rev. 137, A95 (1965).

[7]J. S. Langer, J. Math. Phys. 2, 584 (1961); Phys. Rev. 120, 714 (1960); Phys. Rev. 124, 1003 (1961); Phys. Rev. 127, 5 (1962); Phys. Rev. 128, 110 (1962).

[8]If the frequency spectrum is absolutely continuous (Ref. 2) and if one is in the regime of a well-defined mean free path $l(\omega)$, then a physical argument [see, for example, P. G. Klemens, in *Solid State Physics*, edited by F. Seitz and D. Turnbull (Academic, New York, 1958), Vol. 7, pp. 1–98], can be made for the low-frequency modes which gives an infinite thermal conductivity. The mean free path is given, for low-frequency phonons, by Fermi's Golden Rule $l(\omega) = v_s \tau(\omega) \sim \omega^2/[V^2\, \rho(\omega)]$, where v_s is the velocity of sound, V is the scattering term [as in a generalization of Eq. (3a) below], and $\rho(\omega)$ is the density of states. For low-frequency phonons the scattering potential V varies as $V \sim \omega^2 + O(\omega^3)$, so that we have $l(\omega) \sim 1/[\omega^2 \rho(\omega)]$. Thus, the thermal conductivity $K \sim \frac{1}{3}\int_0 C(\omega) v_s l(\omega)\, d\omega \sim \int_0 \rho(\omega) v_s/[\omega^2 \rho(\omega)]\, d\omega \to \infty$. This result is independent of the dimension of the harmonic system as long as there are only localized scattering centers. When the frequency spectrum has no absolutely continuous part this argument does not hold but it seems that K still diverges for large N, but less rapidly (Ref. 2).

[9]P. G. Klemens, Phys. Rev. 119, 507 (1960); V. Ambegaokar, Phys. Rev. 114, 488 (1959).

[10]R. J. Hardy, Phys. Rev. 132, 168 (1963).

[11]D. N. Zubarev, Usp. Fiz. Nauk 71, 71 (1960) [Soviet Phys.-Usp. 3, 320 (1960)].

[12]D. W. Taylor, Phys. Rev. 156, 1017 (1967).

[13]P. Soven, Phys. Rev. 156, 809 (1967).

[14]B. Velicky, Phys. Rev. 184, 614 (1969); P. L. Leath, Phys. Rev. B 2, 3078 (1970).

[15]H. Mori, I. Oppenheim, and J. Ross, in *Studies in Statistical Mechanics*, edited by J. DeBoer and G. E. Uhlenbeck (Interscience, New York, 1962), Vol. I.

[16]K. R. Allen and J. Ford, Phys. Rev. 176, 1046 (1968).

[17]G. N. Lance, *Numerical Methods for High Speed Computers* (Iliffe, London, 1960), pp. 134–138.

[18]G. Gilat and L. J. Raubenheimer, Phys. Rev. 144, 390 (1966).

PHYSICAL REVIEW B VOLUME 7, NUMBER 6 15 MARCH 1973

Auger-Plasmon-Satellite Intensities versus Depth—A Means for Determining Adatom Concentration Profiles

Peter J. Feibelman*

Department of Physics, State University of New York at Stony Brook, New York 11790

(Received 28 September 1972)

Exit-angle-dependent and angle-integrated Auger-plasmon-satellite intensities are calculated as a function of depth of the Auger emitter into a (Jellium) metal substrate, and as a function of Auger-line energy. The use of measurements of such intensities is proposed as a means of determining the concentration of adatoms versus atomic layer in adsorption experiments.

I. INTRODUCTION

One of the main obstacles to the development of a reliable surface crystallography is that there is usually no way of breaking a surface-structure analysis into a gross part and a detailed part. Questions which are easy to resolve in the case of bulk crystallography, such as the number of atoms per unit cell, are completely nontrivial in the case of surfaces.

Of the gross structural properties that are important in understanding adsorption experiments, we focus here on the adatom concentration versus depth. Typically, in performing an adsorption experiment, after adsorbate gas is admitted to the vacuum chamber, one heats the substrate to bring the system to equilibrium. During this heating, however, adatoms move not only laterally, but also penetrate the surface, assuming some favorable (unknown) distribution in the direction normal to it. In principle this distribution can be determined via an analysis of low-energy-electron-diffraction (LEED) I-V curves taken on the adsorbate-substrate system. However, such LEED data are notoriously difficult to analyze. The author's general approach,[1] therefore, has been to investigate the possibility of determining adatom concentration versus depth by observing decay processes whose probability of occurrence is sensitive to adatom position relative to a surface.